Arabian Journal for Science and Engineering
https://doi.org/10.1007/s13369-024-09915-5

RESEARCH ARTICLE-CHEMICAL ENGINEERING

Preparation of RGO with Enhanced Electrical Conductivity: Effects of Sequential Reductions of L-Ascorbic Acid and Thermal

Dilek Öztekin[1] · Hüseyin Arbağ[1] · Sena Yaşyerli[1]

Received: 29 April 2024 / Accepted: 22 December 2024
© The Author(s) 2025

Abstract
This study aimed to prepare reduced graphene oxide (RGO) with high electrical conductivity by changing the reduction sequences with environmentally friendly L-ascorbic acid and H_2 at moderate temperature. Graphene oxide (GO) was prepared by the modified Hummers method using graphite. The characteristic peak at about 2θ:10° was observed in the XRD pattern, and the oxygen-containing functional groups determined by FTIR analyses indicate the successful preparation of graphene oxide (GO) In order to investigate the removal of oxygen-containing functional groups from GO and the restoration of the graphene structure, XRD, ATR-FTIR, XPS, and Raman analysis were performed. Also, SEM images were taken to see the change in the morphology of the materials. Electrical conductivity measurements of prepared GO and RGO materials were performed using the four-point probe method. RGO-AA-T material, to which first chemical and then thermal reduction is applied, was found to have the highest electrical conductivity value of 1.97×10^4 Sm^{-1} with the highest ratio of C/O:15.5 among other RGOs. XRD and Raman analysis results showed that the initial application of chemical reduction allowed the formation of fewer graphene layers and denser sp^2 domains responsible for the highest electrical conductivity among other materials. The sequence of chemical and thermal treatment significantly enhances the electrical conductivity of RGO by effectively removing oxygen functional groups, maximizing the restoration of sp^2 domains, and preserving structure. These results indicate that the chemical and thermal reduction sequence is very important in improving electrical conductivity. The chemical and thermal reduction applied in this study is a very promising method, and ten times higher electrical conductivity can be achieved compared to the literature.

Keywords Electrical conductivity · Reduced graphene oxide · Ascorbic acid · Thermal reduction

1 Introduction

Graphene is expressed as a material with a flat, two-dimensional, hexagonal lattice structure of carbon having sp^2-hybridized C–C bonding with π-electron clouds [1]. Graphene is a unique material that has attracted the attention of researchers in recent years due to its high strength, flexibility, thermal conductivity, excellent electrical conductivity, and high optical transmittance [2–5]. Its electrical conductivity is reported to be better than copper [2, 6]. Graphene oxide (GO) and reduced graphene oxide (RGO) are the most preferred types of graphene to investigate for use in different technology fields such as energy, sensor fabrications, and nano-electronic devices [7]. It was stated that the number of graphene layers, defect density, crystallite sizes of graphitic domains, and presence of functional groups/dopant atoms are known as important fundamental parameters to determine the quality of graphene-based materials [8]. Graphene oxide is based on the oxidation of graphite with strong acids and oxidants [9]. The modified Hummers method, which is simple, harmless, and safe, has been preferred more in the production of graphene oxide [10–12]. In the modified Hummers method, graphene oxide is generally prepared by adding functional groups (such as hydroxy, epoxy, carboxy, and alkoxy) containing oxygen to the structure [13]. Strong acids such as H_2SO_4, H_3PO_4, and $KMnO_4$ can be used to

✉ Sena Yaşyerli
syasyerli@gazi.edu.tr

Dilek Öztekin
dilekoztekin34@gmail.com

Hüseyin Arbağ
harbag@gazi.edu.tr

[1] Department of Chemical Engineering, Engineering Faculty, Gazi University, 06570 Ankara, Türkiye

Published online: 09 January 2025

form oxygen-containing functional groups [10, 12]. In the literature, graphite particle size, KMnO4 amount and contact time, acid type, and exfoliation conditions are studied as parameters affecting product properties in the preparation of graphene oxide by the modified Hummers method [10, 14].

Reduced graphene oxide (RGO) is prepared as a result of the removal of oxygen-containing functional groups in GO by the reduction process [15]. The reduction process has a significant effect on many properties of the RGO, such as its number of layers, morphology, degree of oxidation, and electrical conductivity. Thermal reduction, chemical reduction, and a combination of them have been generally applied to produce RGO from GO [16–19]. Thermal reduction is an effective method based on heat treatment in reducing or inert atmospheres [20]. The critical parameters in thermal reduction are the selection of reducing environment (H_2 or inert gas), temperature, and period [21]. RGO production was studied at relatively low temperatures (400 °C >) by using H_2 gas as a reducing medium [22]. Reduction at high temperatures (~ 1000 °C) is usually done in inert environments such as Ar [23]. It is stated that the oxygen-containing functional groups in the structure cannot be completely removed by only thermal reduction at high or low temperatures [24]. In addition, the high energy requirement of the reduction process at high temperatures is a vital drawback [5]. In the literature, studies using chemicals as reducing agents are intensely available in the preparation of RGO by reducing GO, with low-cost and large-scale application. Chemical agents with antioxidant and/or oxygen-scavenging properties play an essential role in the removal of oxygen-containing functional groups such as epoxy, carboxyl, and hydroxyl. Chemical reduction of GO can be achieved using Al/HCI, Fe, hydrazine hydrate, hydriodic acid, and natural antioxidants such as lemon grass extract, carrot, Aloe vera juice, and ascorbic acid [25]. In many studies, hydrazine hydrate has been preferred as a reducing agent in the production of RGO, despite its environmental damage. Ascorbic acid attracts researchers' attention as a reducing agent due to its ease of use and environmental friendliness [26]. The literature includes limited studies in which chemical reduction and thermal reduction are used together to increase or optimize electrical conductivity [20, 27–29]. To produce a more functional RGO with fewer structural defects, a series of reduction steps were used in the study of Suranshe and Patil. They investigated water (W)-based reduction, hydrothermal (H) reduction, and microwave (MW) reduction to improve the electrical conductivity of reduced graphene oxide. It was stated that the sequence of reduction methods (W, H, MW) greatly affected its electrical conductivity, and the sequence of W-H-MW reduction gave the highest among them [16]. Thakur et al. found the electrical conductivity 3–4 $\times$ 10^{+3} S m^{-1} by chemical reduction method using an aqueous phytoextract agent [30]. Gao et al. proposed a mechanism for the reduction of graphene oxide using vitamin C and amino acids and stated that this issue is still open to discussion. They proposed a mechanism consisting of two-step S_N2 nucleophilic and subsequent thermal elimination between L-ascorbic acid and graphene oxide. In the reduction mechanism, L-ascorbic acid can separate two protons as a nucleophile with its more acidic hydroxyls. In this mechanism, epoxy and hydroxyl groups in graphene oxide also act as reactive species. The details of the proposed mechanism for the reduction with L-ascorbic acid are available in the study of Gao et al. [31].

Sieradzka et al. (2020) used a thermal reduction chamber blown with N_2 for reduction and reported an electrical conductivity value of 1.407 $\times$ 10^3 S m^{-1} [21]. Deemer et al. (2017) measured the electrical conductivity (5.26 $\times$ 10^1 S m^{-1}) of chemically reduced graphene oxide using L-ascorbic acid [32]. Rozada et al. (2013) investigated chemical (hydrazine monohydrate) and then thermal (under argon flow over 1500 °C) reduction effects on structural changes and electrical conductivity. They investigated the effect of thermal reduction temperature on the electrical conductivity of reduced graphene oxide [33]. Sadek et al. (2022) obtained electrical conductivity results of 1.575 $\times$ 10^3 S m^{-1} in their study with chemically reduced under with a mild and controllable thermal treatment under vacuum at 200 °C [34]. In modern chemistry and materials science, reducing oxygen content is a critical strategy for improving material performance. In the literature, different deoxygenation methods have been reported. Namely, hydrogenation or hydrodeoxygenation (HDO) in catalytic processes plays essential roles in reducing oxygen content. The removal of oxygen can be achieved by combining decarbonylation, decarboxylation, and hydrodeoxygenation reactions to form H_2O, CO, and/or CO_2 [35–37]. The reduction method applied to carbon-based materials such as RGO is very important in terms of preserving the structural properties. Reduction is expected to enhance electron flow between carbon layers and promote more π–π conjugation within the structure, thereby increasing electrical conductivity [21, 34]. These studies illustrate that the reduction method can significantly impact the electrical conductivity of RGO. In a study emphasizing the relationship between electrical conductivity and catalytic activity, the effects of adding highly conductive materials SnO_2 and ZrO_2 and nonconductive MgO to the catalyst by different preparation methods were investigated. It was reported that the addition of SnO_2 increased the catalytic activity due to its high conductivity [38].

To the best of our knowledge, a limited number of studies have been conducted in the literature to improve electrical conductivity. However, studies on this subject continue with the realization that the electrical properties of monolayer graphene having competitive features can be improved. The innovative aspect of this work is the investigation of the effects of sequential chemical and thermal reduction to

improve the electrical conductivity of RGO. In the present study, the focus is on improving the electrical conductivity property of reduced graphene oxide without harming the environment. For this purpose, environmentally friendly L-ascorbic acid and partially medium temperature-H_2 were used for chemical and thermal reduction processes, respectively. There is no similar study in the literature search that primarily addresses the combination of these two methods. For this purpose, graphene oxide was first prepared by the modified Hummers method. Then, reduced graphene oxide was prepared from graphene oxide by using an environmentally friendly ascorbic acid as a chemical reducing agent, thermal reduction with H_2 at medium temperature, and their sequential combinations (chemical + thermal, thermal + chemical).

2 Experimental Method

2.1 Preparation of Graphene Oxide (GO)

In this study, graphene oxide was synthesized using a modified Hummers method [39]. Initially, an acidic mixture was prepared by mixing sulfuric acid (H_2SO_4, 95%-97%, Aldrich) and phosphoric acid (H_3PO_4, 85%, ISOLAB) in a volume ratio of 9:1. Graphite powder (< 150 μm, 99.99%, Aldrich) was added to this mixture. Mixing was continued for 5 min at room temperature. Solid potassium permanganate ($KMnO_4$, > 99%, Atabay) was added to the suspension as an oxidizer. The mixing was continued for a reaction time of 48 h, and a green-colored mixture was obtained. Hydrogen peroxide (H_2O_2, 35%, ISOLAB) was added dropwise to the solution while stirring. The exothermic reaction occurs and is allowed to cool down. Washing was done by adding a mixture of acid (HCl) (37%, Sigma-Aldrich) and deionized water. The mixture was vacuum filtered. The washing and filtration processes were repeated several times. The filtered sample was dried in an oven at 90 °C for 24 h.

2.2 Preparation of Reduced Graphene Oxide (RGO)

In this work, the reduction processes were carried out using the combinations of thermal and chemical reduction steps. Within the scope of the study, the sequence of chemical and thermal applications was changed. The sample that first underwent thermal treatment followed by chemical treatment in the reduction process was named RGO-T-AA. In the reverse sequence reduction process (chemical + thermal), the sample was named RGO-AA-T. In the case of only thermal and only chemical reduction, the samples were named RGO-T and RGO-AA, respectively.

Thermal Reduction Graphene oxide was carried out under 20 ml/min H_2 gas flow at 450 °C with a heating rate of 10 °C/min for 1 h in a tube furnace [40].

Chemical Reduction 0.5 g of GO sample was added to 100 ml of deionized water. 5 g of ascorbic acid (99%, Merck) was added to the solution. The solution was stirred at 60 °C and 600 rpm for 24 h. The suspension was washed several times with deionized water and vacuum filtered. The obtained sample was dried at room temperature. The details of the chemical process are reported in the study of Tewatia et al. [7].

2.3 Characterization Studies

The structural bonds and functional groups of the samples were investigated by Fourier-transform infrared spectroscopy (FTIR) in the medium infrared region of 4000–400 cm^{-1} with a high resolution (4 cm^{-1}) in a Jasco 4700 spectrophotometer. Solid crystalline phases of the prepared samples were determined by the wide-angle (2°–90°) X-ray diffraction (XRD) analysis (Rigaku Ultima-IV diffractometer) with Cu Kα radiation (λ = 0.15406 nm, 40 kV, and 30 mA) and at 2°/min scanning rate. The Raman spectra of the samples were recorded in a Bruker FRA 106/S spectrometer using a 532-nm laser. X-ray photoelectron spectroscopy (XPS) analyses were performed in a SPECS EA300 instrument. SEM analysis was determined using QUANTA 400F field-emission scanning electron microscope (FE-SEM, 30 kV) equipment. The electrical conductivity of prepared materials (GO and RGOs) was measured using an FPP-470 four-point probe (Entek Electronic).

3 Results and Discussion

3.1 Structural Properties of GO and RGO

Figure 1a shows XRD patterns of graphene oxide (GO) prepared by the modified Hummers method, RGO-T (reduction by thermal), RGO-AA (reduction by chemical), and RGO-AA-T (reduction by chemical and thermal). A sharp (2θ:26.41°) and a small (2θ:54.46°) characteristic peaks were observed in the XRD patterns (not shown here) of the graphite used as the starting material (JCPDS Card no:75-1621) [41, 42]. As a result of the oxidation of graphite, the characteristic XRD peaks of graphite disappeared in its XRD patterns. The new two peaks appeared in the XRD pattern of graphene oxide prepared using the modified Hummers method. The new XRD peaks at 2θ:9.97° and 2θ:42.49° in the GO sample indicated the formation of graphene oxide structure in the bulk phase. After different reduction methods, the disappearance of GO's characteristic peak at around 2θ: ~ 10° was observed in the XRD patterns of all RGO materials. The new

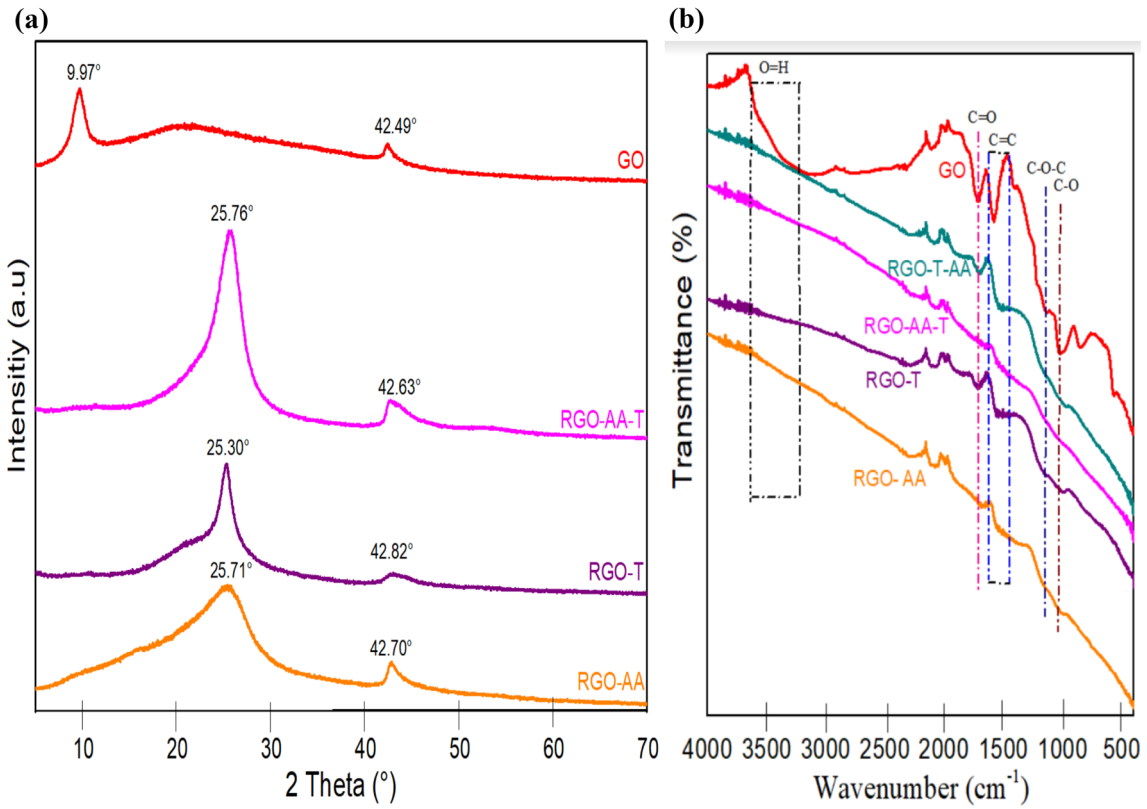


Fig. 1 **a** XRD patterns and (**b**) ATR-FTIR spectra of graphene oxide and reduced graphene oxide materials

Table 1 Results of XRD and Raman analysis of graphite, GO, and RGO materials

Material	Reduction by	d (nm)	FHWM β (°)	L_c* (nm)	L_a*(nm)	N	I_D/I_G
Graphite	–	$0.37_{(002)}$	0.34	23.8	-	70	-
GO	–	$0.91_{(002)}$	1.57	5.0	18.1	6	0.80
RGO-AA	Chemical	$0.35_{(002)}$	6.58	1.2	12.8	4	0.90
RGO-T	Thermal	$0.35_{(002)}$	1.57	5.2	4.3	15	0.83
RGO-AA-T	Chemical + thermal	$0.35_{(002)}$	3.26	2.5	6.8	7	0.98
RGO-T-AA	Thermal + chemical	–	–	–	–	–	0.88

*Using the Scherrer's equation

wide peak at around 2θ:25.5° occurred in the XRD patterns of RGO-T, RGO-AA, and RGO-AA-T. First, XRD results indicated that four different reduction methods successfully prepared reduced graphene oxide materials [23]. Detailed XRD analysis results are given in Table 1. Graphene is generally thought of as a monolayer of sp^2 bonded carbons in a two-dimensional lattice. The carbon layer plane sizes, L_a and L_c, can be estimated using Scherrer's equation. It is called L_c mean crystallite length along the c-axis (also expressed as the height of GO and RGOs stacking nanolayers, H, nm) and is calculated using 002 reflection and 0.9 for the K value. L_a is the mean crystallite length along the a-axis (also expressed as the average diameter of stacking nanolayers, D, nm) and is calculated using two-dimensional (10) reflection and 1.84 for the K value [43–45]. A significant decrease in the L_c size of GO prepared with modified hummers is observed compared to graphite (Table 1). The average number of graphene planes can be estimated using L_c and its corresponding reflection. While the average number of layers (N) was estimated at approximately 70, it significantly decreased to 6 in GO after the oxidation process (Table 1). As well known, the graphene properties strongly depend on the independent number of layers and the defects present in layers. Lc, mean crystallite length along the c-axis, can be preferred to estimate basal

plane oxidation. The decrease in both L_c and N in GO material can express the basal plane oxidation. Chowdhury et al. reported a mechanism for GO formation from graphitic precursors. They explained that basal plane oxidation forms strain in sheets due to the change in hybridization of carbon atoms from sp^2 to sp^3. They emphasized the use of a longer a-axis graphite precursor to produce a long single layer of graphene [44]. In this study, sequential reduction processes were applied to remove the oxygenated functional group from GO to enhance electrical conductivity. Initially, it can be compared to single reduction treatment, thermal and chemical. After thermal reduction, L_c value is similar to GO's value. However, there is an increase in the number of layers of RGO-T. However, L_c value of RGO-AA is smaller than GO's. These results showed that reduction with ascorbic acid was more successful in removing oxygenated groups in the basal plane and preserving the structure. In the application of sequential chemical and thermal treatment, the approximate L_c size was estimated to be 2.5 nm, and the L_a size was estimated to be 6.8 nm. It seems that thermal treatment also affects the decrease in L_a size. The decrease in L_a size indicates the existence of a shorter c-axis. It is important to remember that electrical conductivity also depends heavily on the preservation of structure during reduction. In the study of Kumar and Thakur, they reported that graphene has a strong hydrophilic character due to oxidation with oxygenated functionalities bearing on the edges and basal planes. Due to the presence of oxygen-containing functional groups, GO sheets are a mixture of sp^2 and sp^3 domains of a carbon atom [46]. A similar situation was reported in Chowdhury's study given above [44]. This situation results in low electrical conductivity. Oxygen-functional groups are mostly removed in the RGO preparation by reduction of GO and the hexagonal network of the graphene lattice can be restored. Thus, the electrical conductivity of graphene oxide is significantly recovered.

Fourier-transform infrared spectroscopy (FTIR) analysis has been widely used in numerous studies to successfully identify organic polymers and functional groups, such as HCO_3, CO_3, COOH, CO* [47–49]. In this study, ATR-FTIR study was carried out to compare the surface functional groups on the synthesized GO and RGO materials (Fig. 1b). The functional groups on the surface that can be found in GO depend strongly on the method of preparation and graphite properties. The broad peak observed in the region of approximately 3300–3850 cm^{-1} in the FTIR spectrum of the GO belongs to the -OH group due to the presence of some water molecules. In the structure of porous organic polymers (TPT-POP), peaks observed around ~ 3420 cm^{-1} confirm the presence of hydroxyl (OH) groups [47]. For the same material, peaks belonging to the carboxyl (for C = O stretching vibrations), aromatic bond (C = C, non-oxidized carbon), epoxy (C–O–C stretching vibrations), and alkoxy (C–O stretching vibrations) groups are observed at about 1718, 1577, 1148, and 1020 cm^{-1} bands, respectively. Epoxy (-O-), hydroxyl (-OH), carbonyl (-C = O), carboxyl (-COOH), and alkoxy (C-O) in GO are mainly mentioned as oxygen-containing functional groups in the literature [6, 15, 32, 50]. It is also reported that epoxy and hydroxyl groups are located on its basal plane as major components. Carbonyl and carboxyl, minor components, are distributed at its layer edges [51]. However, in the review study of Padamata et al., it was reported that the carboxyl group (~ 1718 cm-1) was in the basal plane of graphene [52]. In their study, Gao et al. stated that the oxygen-containing functional groups on the basal plane are easier to remove than those in the defective sites or edges [29]. When ATR-FTIR spectra of GO and RGO materials are compared, changes in surface functional groups are observed in Fig. 1b. In all the RGO materials, the hydroxyl groups (-OH) observed at 3300–3850 cm^{-1} disappeared due to the formation of hydrophobic nature of reduced graphene oxide formed after reduction (Fig. 1b). The characteristic aromatic (C = C) peak in all RGO materials was observed as small and broad in the wavenumber range of 1560–1561 cm^{-1}. Peak intensities of carboxyl groups are observed slightly higher in FTIR spectra of materials prepared by thermal and thermal + chemical reduction only when compared to materials prepared by the other two reduction methods. Therefore, FTIR analyses show that more carboxyl groups were removed in processes with chemical reduction. However, peaks belonging to the epoxy group disappeared in all RGO materials. While the C-O belonging to the alkoxy functional group is observed to be quite small in the FTIR spectra of reduced graphene oxides (RGOs), it is almost absent in RGO-AA-T material. It can be concluded that the functional groups containing oxygen were mostly removed by the combination of chemical + thermal reduction process. This situation supported the conclusion that a single reduction is not sufficient to remove more oxygen-containing functional groups [19].

The Raman spectroscopy is carried out to analyze structural disorder in more detail after reduction. In the Raman spectrum, the G (at around 1598 cm^{-1}, graphitic, sp^2) and the D (at around 1351 cm^{-1}, defects or edge planes, sp^3) bands are associated with interlayer stretching vibrations of C–C and structural defects, edge effects, or disorder in carbon material as a result of oxidation of graphite, respectively [32, 53, 54]. A strong D band, often stronger than the G band, reveals the presence of a large number of defects. After reduction, the content of sp^2-hybridized carbon atoms is expected to increase, giving an increase in the area of the graphene domains. Also, the D band generally indicates the formation of vacancies and grain boundaries due to the structure defects in the carbon material [32]. The 2D band gives information about the number of layers [55–58]. The relative intensity ratio of I_D/I_G is expected to increase in reduced

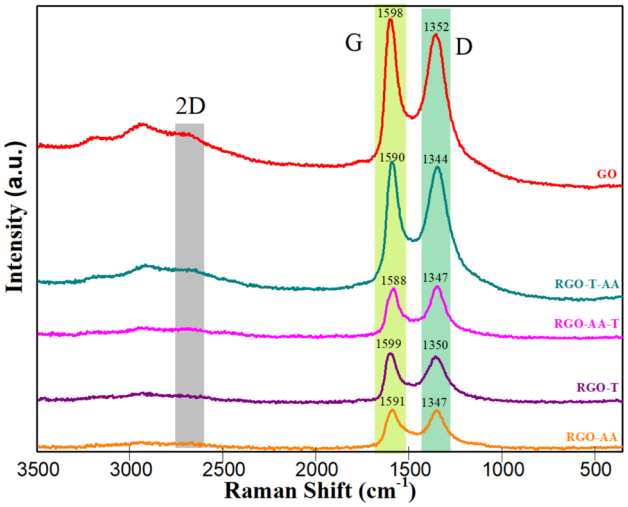


Fig. 2 Raman spectra of GO, RGO-AA, RGO-T, RGO-AA-T, and RGO-T-AA materials

graphene oxide due to the decrease in the sp3 carbon fraction and sp^2 carbon re-buildings [20, 25, 59, 60]. In other words, the increase in the I_D/I_G ratio indicates the formation of sp^2 structures and the reduction of functional groups [60]. In the Raman spectra of all GO and RGO materials, D and G bands were clearly observed in Fig. 2. The D and G bands of GO material are located at around 1352 cm^{-1} and 1598 cm^{-1}, respectively. The intensity ratio (I_D/I_G) of the D to G peak for GO was determined as 0.80 (Table 1). The values of I_D/I_G ratios were increased to 0.83, 0.90, 0.98, and 0.88 for reduced materials using thermal, chemical, chemical + thermal, and thermal + chemical reduction methods, respectively. The shift in the D and G bands in the Raman spectra can provide information about the number of layers in the literature [15, 46]. They stated that significant red shift in the G band for reduced GOs indicated a decrease in the number of layers after reduction. In this study, the location of G bands in the RGO-AA and RGO-AA-T materials shifted to a lower wavenumber, namely; 1591 cm^{-1} and 1588 cm^{-1}, respectively [15]. In light of all this information, the shift in the peak indicates a successful reduction of graphene oxide and may lead to an increase in electrical conductivity [61]. The increase in the ratio of I_D/I_G showed that sp^2 carbon re-buildings after reduction.

$$L_a = 4.35 \left(\frac{I_D}{I_G}\right)^{-1} \quad (1)$$

It is believed that the sp^2 carbon area is another important criterion in the electronic properties of carbon materials. The Knights equation shown in Eq. 1 is used to estimate the average crystallite size of sp^2 domains (carbon diameter = L_a) using the intensity ratio (I_D/I_G) of the D and G peaks. The decrease in crystallite size shows that the sp^2 density increases due to the formation of sp^2 carbon domains transformation of sp^3 during the reduction process. The decrease in crystallite size is an indication that the defects are also reduced [61–63]. Carbon diameter (L_a) of GO, RGO-AA, RGO-T, RGO-AA-T, and RGO-T-AA materials were calculated as 5.44 nm, 4.86 nm, 5.21 nm, 4.45 nm, and 4.92 nm, respectively (reported in Table 2). Considering L_a value of all RGO, the best reduction was achieved with RGO-AA-T prepared by the chemical + thermal reduction method. As a result, small crystallite size has been reported as an indicator of successful reduction in the literature. Also, for carbon-related materials, the average crystallite size and I_D/I_G ratio are reported as inversely proportional to the average crystallite size [15]. In this study, while the RGO-AA material had the smallest crystallite size (L_c) of 1.2 nm, the I_D/I_G value was determined as 0.90. The RGO-AA-T material with a slightly larger crystallite size (2.5 nm) has the highest I_D/I_G (0.98) among others. The successful synthesis of RGOs was also supported by the decrease in sp^2 carbon diameter. The reduction in the crystallite size of the sp^2 carbon field indicates that dense sp^2s are formed in RGOs compared to GO [62]. First ascorbic acid and then thermal reduction caused a reduction in the average size of the graphitic domains due to small re-graphitization. However, this is not the case with the material prepared first by thermal and then by reduction with ascorbic acid. In this study, a broad and low-intensity peak is observed in the 2D region at approximately 2600 cm^{-1}, showing the formation of multilayered GO materials. The observation of a very broad and small peak in the 2D region of the Raman spectrums of the RGO-T and RGO-T-AA materials shows that the multilayer is present even after reduction [64]. XRD analyses of the RGO-T material also confirm the formation of a multilayer ($N \cong 15$).

The surface chemistry, especially oxygen-containing functional groups of graphene oxide and reduced graphene oxide materials, was also investigated with XPS analysis precisely. In a comprehensive study by Trinh et al., the C1s binding energy for well-characterized carbon species on Co (0001) and Ni (100) was determined by XPS and the results were compared with density functional theory (DFT) calculations. It was stated that the combined use of (XPS) and (DFT) calculations allows for a more accurate interpretation of core-level binding energy shifts and surface species [65, 66]. XPS spectra of GO and all RGO materials are presented in Fig. 3. The success of the reduction process largely depends on the removal of the surface oxygen groups, but it is important that it does not damage the basal planes while doing so. XPS analysis showed that while the carbon in the GO material was determined as 57% (atomic), after the reduction process, that of the RGO-T-AA and RGO-AA-T materials reached 82.3% and 91.1%, respectively. XPS also determined the surface ratios of C/O of GO, RGO-AA, RGO-T, RGO-AA-T, and RGO-T-AA as 1.59, 3.57, 5.86, 6.62, and

Table 2 Electrical conductivities and characteristic properties of GO and RGO materials

Material	Preparation method	C/O (Atomic) by XPS	L_a (nm) by Raman	Electrical conductivity (S m^{-1})
GO	Modified Hummers	1.59	5.44	4.56×10^{-2}
RGO-AA	Chemical reduction	3.57	4.86	4.23×10^{3}
RGO-T	Thermal reduction	5.86	5.21	6.76×10^{3}
RGO-AA-T	Chemical + thermal reduction	15.5	4.45	1.97×10^{4}
RGO-T-AA	Thermal + chemical reduction	6.62	4.92	6.71×10^{3}

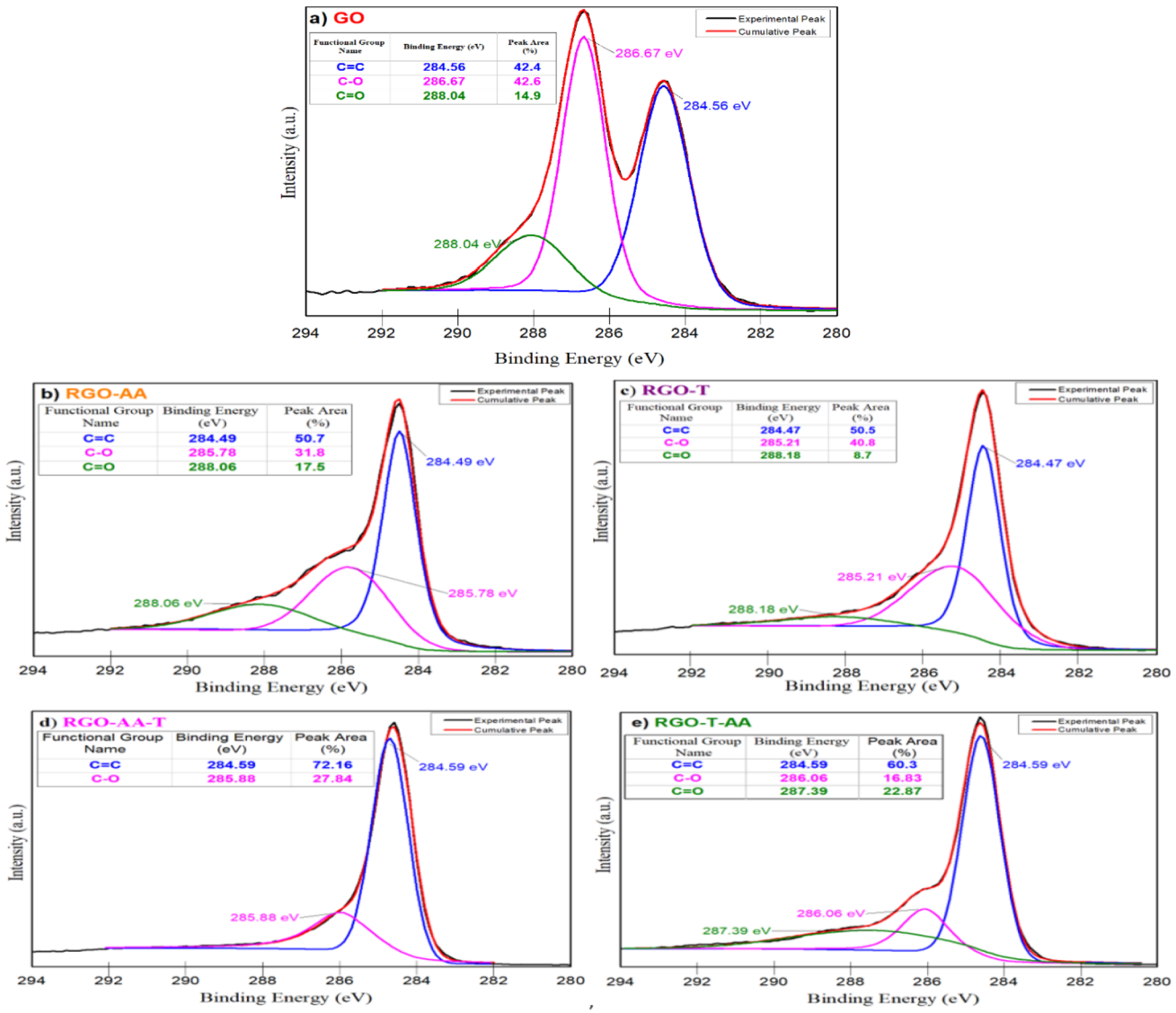


Fig. 3 XPS spectra of **a** GO, **b** RGO-AA, **c** RGO-T, **d** RGO-AA-T, **e** RGO-T-AA materials

15.5, respectively. It is clearly seen that the removal of oxygen groups has been achieved by reduction processes with environmentally friendly ascorbic acid and H_2 flow at relatively low temperatures. Considering the single reduction method, it is observed that only thermal reduction (C/O: 5.86) is more successful than only chemical (C/O: 3.57) reduction. The C/O ratio was slightly increased (C/O: 5.86 $\rightarrow$ 6.62) when chemical reduction was applied after thermal reduction. However, a significant increase (C/O: 3.57 $\rightarrow$ 15.5) was observed in the C/O ratio when the process sequence was changed. Therefore, the increase and change in the C/O ratio after all reduction processes indicate that the oxygen-containing functional groups have been removed, as expected. The increase in C/O ratios in RGO-AA-T and RGO-T-AA shows that the sequence of the chemical and thermal reduction is very crucial to removing oxygen-containing functional groups. To find percentages of carbon–oxygen species on the surface of GO and RGO materials, the deconvolution analysis of the C1s peak (284.5 eV) was performed. The deconvolution analysis shows three peaks in the C1s spectrum of the GO sample. These peaks were evaluated as the C = C (non-oxygenated ring carbon) bond at 284.56 eV, the C–O (epoxy and/or hydroxyl groups) bond at 286.67 eV, and the C = O (carbonyl carbon) bond at 288.04 eV (Fig. 3a). Deconvolution analysis indicates that the highest C = C structure is in RGO-AA-T material. When only thermal and chemical reductions were compared, C–O and C = O groups were still detected in both structures despite the proportional differences. The deconvolution analysis of C1s peak shows the absence of double-bonded carbon–oxygen groups in the RGO-AA-T material and the presence of oxygen in the C–O bond (e.g., epoxy group). In the study of Farah et al., the effect of ascorbic acid and thermal (300 °C, Ar) reduction on the removal of oxygen groups was investigated [27]. Researchers have reported that chemical reduction with ascorbic acid is more effective in removing oxygen groups and causes significant fragmentation of graphene-like sheets.

To see the change in morphology of prepared materials, SEM images of GO, RGO-T, RGO-AA, and RGO-T-AA are presented in Fig. 4. Graphene oxide is expected to occur with the formation of carbon–oxygen bonds with the oxidation of graphite. Thus, different oxygen-containing functional groups are formed in the structure. Carbon–oxygen bonds disrupt the sp^2 conjugate structure and formation of smooth layers consisting of wrinkled; thus, curved areas were formed in GO [40]. A similar observation was seen in the SEM images of GO prepared in this study. As a result of reduction processes, the morphology of reduced materials changed. SEM photographs of reduced graphene oxide materials show the formation of new transparent layers stacked on top of each other and irregularly shaped. A similar observation in the SEM images of RGOs was reported in the study of Khosroshahi et al. [26] and De Silva et al. [53]. When comparing thermal and chemical reduction, larger particles are observed after thermal reduction. Also, while a tighter granular structure is observed with fewer voids and sharp boundaries in RGO-T material, the situation is more dispersed in RGO-AA material. With the application of the thermal + chemical treatment, the particle boundaries were partially obscured, and the SEM photograph of the RGO-T-AA material showed more similarity to that of the RGO-AA material. The chemical reduction using ascorbic acid followed by thermal reduction (RGO-AA-T) may lead to partial restacking and agglomeration of graphene layers with smaller particles due to $\pi-\pi$ interactions and Van der Waals forces between the basal planes. The wrinkled, irregular ball-type morphology observed in SEM images could result from the structural rearrangement and removal of oxygen-containing functional groups during the reduction processes [26, 41, 53, 67].

3.2 Electrical Conductivity of RGO

Graphene has been intensively researched as a potential material for use in many fields (catalyst, energy, sensors) with its thin structure, transparency, flexibility, as well as strong structure, optical, magnetic, and electronic properties [6, 32]. As known, graphene can be defined as an independent two-dimensional layer planar of carbon hexagons consisting of sp^2 hybridized bonding with π-electron cloud. The electronic properties of graphene depend on the number of layers, defects present in each layer, chemical composition, and oxidation level [4, 68, 69]. It was reported that the high electrical conductivity of graphene is due to zero-band gap semimetal with electrons and holes as charge carriers [70]. The electrical conductivity of graphene is crucial due to the presence of two π electrons in every hexagon of the graphene layer [4]. To prepare graphene with high electrical conductivity, graphene oxide can be prepared by first introducing some oxygen-containing functional groups into graphite. Thus, the transformation of the graphite structure into the two-dimensional graphene structure is achieved and the distance between layers increases. Next, since the structure has sp^2/sp^3 hybridization, reduced graphene oxide is prepared by containing predominantly sp^2 hybridization, and a low number of layers by removing/reducing oxygen-containing functional groups. During all these processes, care is taken to preserve the graphene structure. This study aims to prepare reduced graphene oxide (RGO) with high electrical conductivity using ascorbic acid as an environmentally friendly chemical and H_2 at low energy consumption. For this purpose, graphene oxide was synthesized by the modified Hummers method using graphite as a starting material. To improve the electrical conductivity property and achieve a high C/O ratio, the reduced graphene oxides were prepared by sequential reduction (chemical + thermal & thermal + chemical) and single reduction (chemically by L-ascorbic

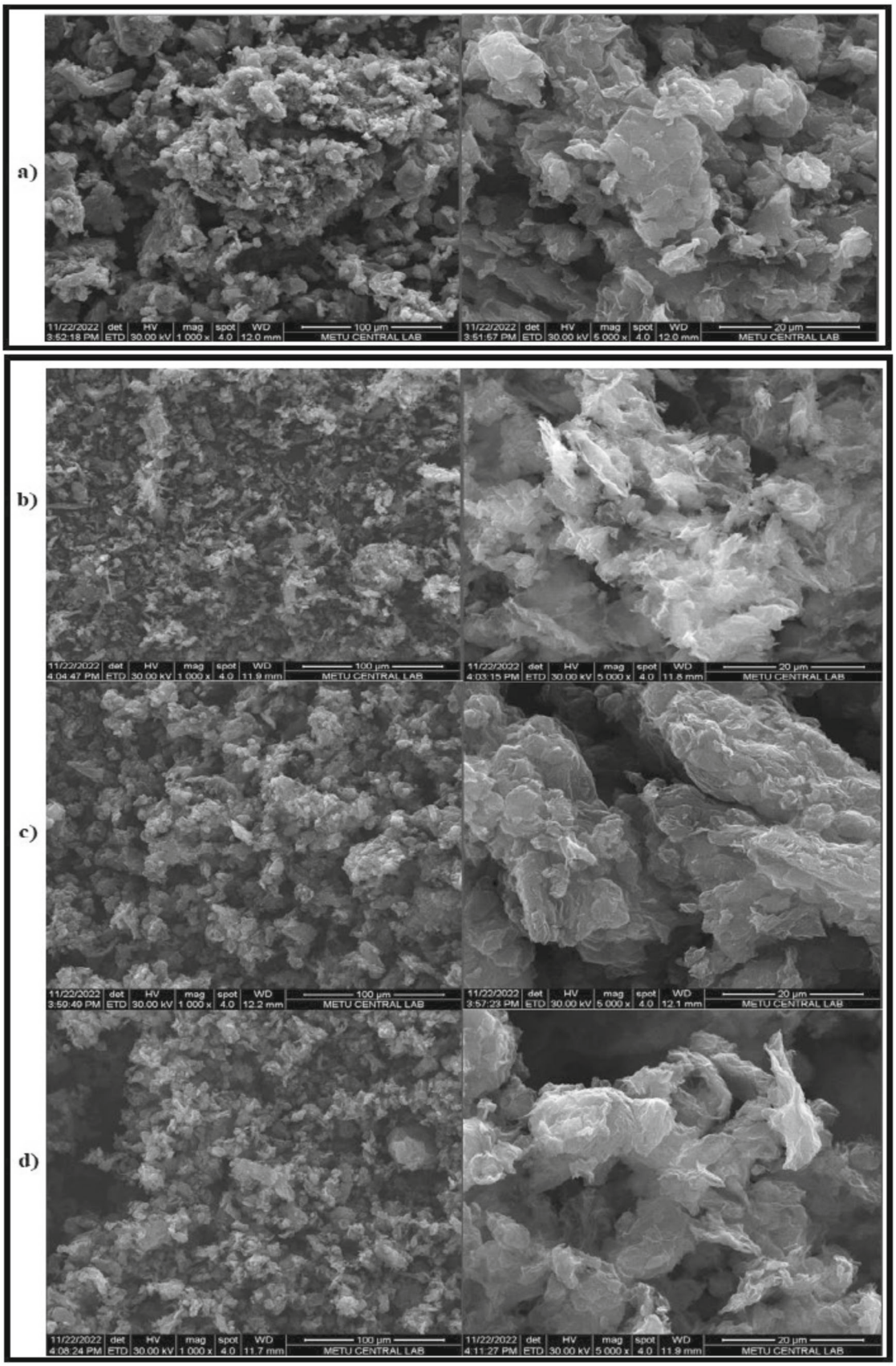


Fig. 4 SEM Images of **a** GO, **b** RGO-AA, **c** RGO-T, **d** RGO-T-AA

acid & thermally at 450 °C, H_2). The four-point probe (FPP) method was used to measure the electrical conductivity of prepared RGO material. Table 2 presents the electrical conductivity of GO and RGO materials and their characteristic properties. The electrical conductivity of RGOs, prepared by chemical and thermal processes, and the combination of chemical and thermal processes significantly increased compared to that of the GO material. The measurements showed that the RGO-AA-T material, which has a C/O:15 value, has the highest electrical conductivity with a value of 1.97×10^4 S m^{-1}, among others. The electrical conductivity of thermally reduced RGO-T was found to be slightly higher than that of chemically reduced RGO-AA, although in the same order of magnitude. The electrical conductivity value of RGO-T-AA reduced with ascorbic acid after thermal reduction is close to that of RGO-T reduced only thermally. The electrical conductivity values and the close C/O ratios of the RGO-T and RGO-T-AA materials show that the chemical treatment does not improve the electrical conductivity if applied after thermal treatment. It is believed that performing thermal reduction first may cause some damage to the basal plane by removing many oxygen-containing functional groups, while single chemical reduction is less effective in improving the electrical properties of graphene. In the study of Tiwari et al., it was stated that thermal effects cause carbon and oxygen to move away from the structure as CO_2, thus causing mass loss and structural degradation [4]. Bychko et al. mentioned that in the reduction in the H_2 environment at 400 °C, the adsorbed water, epoxy and carboxyl groups, and hydroxyl, ether and carbonyl groups are partially removed [54]. In this study, the decrease in carbonyl groups and C/O values was determined to be close to each other after thermal and thermal + chemical reduction. However, the possibility of CO_2 emissions from the structure should also be taken into consideration. Functional group location, namely plane or edge, in graphene is essential in the separation of functional groups. L_c values calculated using XRD data (Table 1) were found to be almost the same for GO and RGO-T materials. The L_a value of the RGO-T material, also referred to as the distance between defects in RGO, was calculated as the lowest. The proximity of defects in the material prepared by thermal reduction may cause a decrease in electrical conductivity as it increases the possibility of scattering of electrons. Also, there are still some oxygen-containing functional groups after thermal reduction. As a result of chemical reduction, the L_a value of the material was obtained close to that of GO. In thermal reduction, the La value of the material is the lowest. Considering that the L_a value is the crystallite length along the a-axis, it can be thought that there may be more edges in the material with a smaller La value as a result of thermal reduction. It may be speculative, but in this case, the remaining oxygen groups in the structure may be at the edges. In addition to deterioration of the structure, this may result in less electrical conductivity. In this study, L-ascorbic acid was used as a chemical reduction agent due to being environmentally friendly. In the literature, hydrazine is a commonly preferred chemical agent [4, 7, 10]. In the case of using hydrazine, in addition to its harm to the environment, there is also the possibility of concomitant introduction of nitrogen atoms during reduction. This may cause minimal N-doping on graphene layers [4]. While Raman analyses show increasing sp^2 domains and graphene re-buildings in the RGO-AA material, XRD analyses show that oxygenated functional groups are removed due to low L_c. The literature says that the increase in I_D/I_G ratio shows the rise in the population of sp^2 domains at the expense of domain size and an increase in defects and sp^2 carbon re-buildings [25, 61]. Rudenko et al. emphasized that the restoration of graphene structure is important in enhancing electrical conductivity [59]. Monolayer graphene has the highest electrical conductivity because it has only two free electron channels [68]. As the number of layers increases, electron scattering will increase and conductivity most probably be negatively affected. The higher number of layers in the RGO-T material may also be the reason for the lower electrical conductivity. XPS analysis results of the same material give a lower C/O ratio. This also shows that with only chemical reduction, less oxygenated groups are removed, and the structure is more preserved. However, thermal reduction after chemical reduction significantly increased the C/O ratio to 15. In SEM photographs, it was observed that relatively larger particles were formed by thermal reduction with more distinct borders. These results may show that thermal effects may cause deterioration in the basal planes of the graphene structure and that the structure is better preserved in reduction with ascorbic acid. This reduction sequence most likely increased the electrical conductivity because it caused the removal of oxygen-containing groups while preserving the structure. However, analysis results showed that chemical reduction alone is insufficient to restore graphene structure.

Studies on the electrical conductivity of reduced graphene oxide in the literature are presented in Table 3. In the literature, electrical conductivity values of reduced graphene oxide were reported at different levels/values. The electrical conductivity values of all reduced graphene oxides obtained in this study are comparable to those reported in the literature. The electrical conductivity value of the RGO-AA-T material was found to be approximately 10 times higher than that of other materials reported in the literature. The high electrical conductivity results from the effective removal of oxygen-containing functional groups that are difficult to eliminate and the greater efficiency in regaining the sp^2 carbon networks crucial for electrical conductivity.

Table 3 Comparison of electrical conductivity values of reduced graphene oxide prepared in this study and the literature

Reduced graphene oxide, Reference	Reduction method	Electrical conductivity measurement	Electrical conductivity ($S\ m^{-1}$)
rH4, [32]	Chemical reduction by AA, NH_4	Four-point probe method	5.26×10^1
HG1500-2700, [33]	Thermal reduction by Ar at 1500–2700 °C	Van Der Pauw method	5.77×10^2
TCRGOL, [34]	Chemical reduction by AA and thermal by reduction under vacuum at 400 °C	Four-point probe method	2.14×10^3
rGO20, [21]	Thermal reduction by N_2 at 300 °C	Four-point probe method	1.41×10^3
CRGO, [30]	Chemical reduction by aqueous phytoextract	Four-point probe method	4.01×10^3
rGO (W-H-MW), [16]	Water, hydrothermal, and microwave reductions	–	4.38×10^1
RGOHCl, [71]	Chemical reduction by hydrochloric acid	Four-point probe method	1.56×10^2
RGO-AA-T, This Study	Thermal reduction by H_2 at 450 °C and chemical reduction by AA	Four-point probe method	1.97×10^4

4 Conclusion

The study aims to prepare reduced graphene oxide (RGO) with high electrical conductivity. For this purpose, the effect of reduction sequences of graphene oxide on its electrical conductivity was investigated. Chemical reduction was carried out using environmentally friendly ascorbic acid, and thermal reduction was carried out at a relatively low temperature of 450 °C in a H_2 gas environment. RGO materials were prepared using the difference sequence of thermal and chemical processes. In order to compare the effect of sequence, only chemical reduction and thermal reduction were applied as well. The properties of the RGO-AA-T material showed that the chemical + thermal sequence was the most successful reduction. With chemical + thermal reduction, it can be concluded that applying the chemical treatment first removes more oxygen-containing functional groups from the structure, allowing for the increase in sp^2 carbon re-buildings and preserving the structure. The electrical conductivity values of the RGOs measured by four-point probe were obtained as comparable with the values in the literature. The electrical conductivity value of RGO-AA-T material with a C/O ratio of 15.5 is $1.97 \times 10^4\ Sm^{-1}$, which is the highest value obtained in this study. It was concluded that the thermal reduction applied after chemical reduction improved the electrical conductivity. This study showed that the sequential chemical and thermal reduction process is an up-and-coming method for preparing graphene with high electrical conductivity.

5 Data and Code Availability

Not applicable.

Acknowledgements Gazi University Research Fund (BAP-FYL-2021-7137) grant is gratefully acknowledged. Thanks are due to Prof. Dr. Bekir Sarı of Gazi University and MSc Student Sedanur Arslan for the electrical conductivity measurements. The authors would like to thank Gazi University Academic Writing Application and Research Center for proofreading the article.

Author Contributions Dilek Oztekin was involved in investigation, validation, writing—original draft; Huseyin Arbag helped in conceptualization, methodology, formal analysis, Sena Yasyerli contributed to conceptualization, methodology, formal analysis, writing—reviewing and editing.

Funding Open access funding provided by the Scientific and Technological Research Council of Türkiye (TÜBİTAK).

Declarations

Conflict of interest There is no conflict of interest.

Ethical Approval Not applicable.

Open Access This article is licensed under a Creative Commons Attribution 4.0 International License, which permits use, sharing, adaptation, distribution and reproduction in any medium or format, as long as you give appropriate credit to the original author(s) and the source, provide a link to the Creative Commons licence, and indicate if changes were made. The images or other third party material in this article are included in the article's Creative Commons licence, unless indicated otherwise in a credit line to the material. If material is not included in the article's Creative Commons licence and your intended use is not permitted by statutory regulation or exceeds the permitted use, you will need to obtain permission directly from the copyright holder. To view a copy of this licence, visit http://creativecommons.org/licenses/by/4.0/.

References

1. Mathur, R.B.; Singh, B.P. (eds): Carbon Nanomaterials: Synthesis, Structure, Properties and Applications. CRC Press, US (2016). https://doi.org/10.1201/9781315371849
2. Takai, K.; Tsujimura, S.; Kang, F.; Inagaki, M. (eds.): Graphene: preparations, properties, applications, and prospects. Elsevier, US (2019)
3. Pradhan, S.S.; Ghosh, T.N.; Marik, A.; Raul, K.K.; Sarkar, S.K.: Magnetodielectric effects in three reduced graphene oxide–polymer nanocomposites. Bull. Mater. Sci. **43**, 208 (2020). https://doi.org/10.1007/s12034-020-02185-5
4. Tiwari, S.K.; Sahoo, S.; Wang, N.; Huczko, A.: Graphene research and their outputs: status and prospect. J. Sci. Adv. Mater. Devices **5**, 14–18 (2020). https://doi.org/10.1016/j.jsamd.2020.01.006
5. Singh, R.K.; Kumar, R.; Singh, D.P.: Graphene oxide: strategies for synthesis, reduction and frontier applications. RSC Adv. **6**, 64993–65011 (2016). https://doi.org/10.1039/C6RA07626B
6. Sharma, D.; Kanchi, S.; Sabela, M.I.; Bisetty, K.: Insight into the biosensing of graphene oxide: present and future prospects. Arab. J. Chem. **9**, 238–261 (2016). https://doi.org/10.1016/j.arabjc.2015.07.015
7. Tewatia, K.; Sharma, A.; Sharma, M.; Kumar, A.: Synthesis of graphene oxide and its reduction by green reducing agent. Mater. Today Proc. **44**, 3933–3938 (2020). https://doi.org/10.1016/j.matpr.2020.09.294
8. Kaushal, A.; Dhawan, S.K.; Singh, V.: Determination of crystallite size, number of graphene layers and defect density of graphene oxide (GO) and reduced graphene oxide (RGO). AIP Conf. Proc. (2019). https://doi.org/10.1063/1.5112945
9. Axet, M.R.; Durand, J.; Gouygou, M.; Serp, P.: Chapter Two - Surface coordination chemistry on graphene and two-dimensional carbon materials for well-defined single atom supported catalysts. Adv. Organomet. Chem. **71**, 53–174 (2019). https://doi.org/10.1016/bs.adomc.2019.01.002
10. Andrijanto, E.; Shoelarta, S.; Subiyanto, G.; Rifki, S.: Facile synthesis of graphene from graphite using ascorbic acid as reducing agent. AIP Conf. Proc. (2016). https://doi.org/10.1063/1.4945457
11. Habte, A.T.; Ayele, D.W.: Synthesis and characterization of reduced graphene oxide (rGO) started from graphene oxide (GO) using the Tour method with different parameters. Adv. Mater. Sci. Eng. **2019**, 1–9 (2019). https://doi.org/10.1155/2019/5058163
12. Kaur, M.; Kaur, H.; Kukkar, D.: Synthesis and characterization of graphene oxide using Modified Hummer's method. AIP Conf. Proc. (2018). https://doi.org/10.1063/1.5032515
13. Tang, S.; Liu, Z.; Xiang, X.: Graphene oxide composite hydrogels for wearable devices. Carbon Lett. **32**, 1395–1410 (2022). https://doi.org/10.1007/s42823-022-00402-1
14. Higginbotham, A.L.; Kosynkin, D.V.; Sinitskii, A.; Sun, Z.; Tour, J.M.: Lower-defect graphene oxide nanoribbons from multiwalled carbon nanotubes. ACS Nano **4**, 2059–2069 (2010). https://doi.org/10.1021/nn100118m
15. Joshi, R.; De Adhikari, A.; Dey, A.; Lahiri, I.: Green reduction of graphene oxide as a substitute of acidic reducing agents for supercapacitor applications. Mater. Sci. Eng. B **287**, 116128 (2023). https://doi.org/10.1016/j.mseb.2022.116128
16. Suranshe, S.S.; Patil, A.: Strategically improving electrical conductivity of reduced graphene oxide through a series of reduction processes. Mater. Lett. **333**, 133648 (2023). https://doi.org/10.1016/j.matlet.2022.133648
17. Xie, L.; Sha, J.; Ma, Y.; Han, J.: Thermal reduction of graphene oxide in organic solvents for producing colloidal suspensions of reduced graphene oxide sheets. Fuller. Nanotub. Carbon Nanostruct. **21**, 901–915 (2013). https://doi.org/10.1080/1536383X.2013.826196
18. Chua, C.K.; Pumera, M.: Reduction of graphene oxide with substituted borohydrides. J. Mater. Chem. A. **1**, 1892–1898 (2013). https://doi.org/10.1039/C2TA00665K
19. Eda, G.; Fanchini, G.; Chhowalla, M.: Large-area ultrathin films of reduced graphene oxide as a transparent and flexible electronic material. Nat. Nanotechnol. **3**, 270–274 (2008). https://doi.org/10.1038/nnano.2008.83
20. Pei, S.; Cheng, H.M.: The reduction of graphene oxide. Carbon **50**, 3210–3228 (2012). https://doi.org/10.1016/j.carbon.2011.11.010
21. Sieradzka, M.; Ślusarczyk, C.; Fryczkowski, R.; Janicki, J.: Insight into the effect of graphite grain sizes on the morphology, structure, and electrical properties of reduced graphene oxide. J. Mater. Res. Technol. **9**, 7059–7067 (2020). https://doi.org/10.1016/j.jmrt.2020.05.026
22. Qiu, Y.; Guo, F.; Hurt, R.; Külaots, I.: Explosive thermal reduction of graphene oxide-based materials: mechanism and safety implications. Carbon **72**, 215–223 (2014). https://doi.org/10.1016/j.carbon.2014.02.005
23. Okutan, M.: Electrochemical determination of ascorbic acid with thermally reduced graphene oxide. J Faculty Eng Archit Gazi Univ. **35**, 1589–1602 (2020)
24. Sharma, A.; Erdenedelger, G.; Jeong, H.M.; Lee, B.K.: Controlled oxygen functional groups on reduced graphene using rate of temperature for advanced sorption process. J. Environ. Chem. Eng. **8**, 103749 (2020). https://doi.org/10.1016/j.jece.2020.103749
25. Verma, S.; Das, T.; Pandey, V.K.; Verma, B.: Facile and scalable synthesis of reduced-graphene oxide using different green reducing agents and its characterizations. Diam. Relat. Mater. **129**, 109361 (2022). https://doi.org/10.1016/j.diamond.2022.109361
26. Khosroshahi, Z.; Kharaziha, M.; Karimzadeh, F.; Allafchian, A.: Green reduction of graphene oxide by ascorbic acid. AIP Conf. Proc. (2018). https://doi.org/10.1063/1.5018941
27. Farah, S.; Farkas, A.; Madarász, J.; László, K.: Comparison of thermally and chemically reduced graphene oxides by thermal analysis and Raman spectroscopy. J. Therm. Anal. Calorim. **142**, 331–337 (2020). https://doi.org/10.1007/s10973-020-09719-3
28. Lavin-Lopez, M.D.P.; Paton-Carrero, A.; Sanchez-Silva, L.; Valverde, J.L.; Romero, A.J.A.P.T.: Influence of the reduction strategy in the synthesis of reduced graphene oxide. Adv. Powder Technol. 28, 3195–3203 (2017). https://doi.org/10.1016/j.apt.2017.09.032
29. Gao, W.; Alemany, L.B.; Ci, L.; Ajayan, P.M.: New insights into the structure and reduction of graphite oxide. Nat. Chem. **1**, 403–408 (2009). https://doi.org/10.1038/nchem.281
30. Thakur, S.; Karak, N.: Green reduction of graphene oxide by aqueous phytoextracts. Carbon **50**, 5331–5339 (2012). https://doi.org/10.1016/j.carbon.2012.07.023
31. Gao, J.; Liu, F.; Liu, Y.; Ma, N.; Wang, Z.; Zhang, X.: Environment-friendly method to produce graphene that employs vitamin C and amino acid. Chem. Mater. **22**, 2213–2218 (2010). https://doi.org/10.1021/cm902635j
32. Deemer, E.M.; Paul, P.K.; Manciu, F.S.; Botez, C.E.; Hodges, D.R.; Landis, Z.; Chianelli, R.R.: Consequence of oxidation method on graphene oxide produced with different size graphite precursors. Mater. Sci. Eng. B **224**, 150–157 (2017). https://doi.org/10.1016/j.mseb.2017.07.018
33. Rozada, R.; Paredes, J.I.; Villar-Rodil, S.; Martínez-Alonso, A.; Tascón, J.M.: Towards full repair of defects in reduced graphene oxide films by two-step graphitization. Nano Res. **6**, 216–233 (2013). https://doi.org/10.1007/s12274-013-0298-6
34. Sadek, R.; Sharawi, M.S.; Dubois, C.; Tantawy, H.; Chaouki, J.: Tolerated reduction protocol of graphene for high performance EMI shielding materials. SSRN. 1–34 (2022). https://ssrn.com/abstract=4045833
35. Sarkar, C.; Shit, S.C.; Dao, D.Q.; Lee, J.; Tran, N.H.; Singuru, R.; Mondal, J.: An efficient hydrogenation catalytic model hosted in a

stable hyper-crosslinked porous-organic-polymer: from fatty acid to bio-based alkane diesel synthesis. Green Chem. **22**, 2049–2068 (2020). https://doi.org/10.1039/C9GC03803E
36. Paul, R.; Shit, S.C.; Fovanna, T.; Ferri, D.; Srinivasa Rao, B.; Gunasooriya, G.K.K.; Mondal, J.: Realizing catalytic acetophenone hydrodeoxygenation with palladium-equipped porous organic polymers. ACS Appl Mater Interfaces (2020). https://doi.org/10.1021/acsami.0c16680
37. Trinh, Q.T.; Banerjee, A.; Ansari, K.B.; Dao, D.Q.; Drif, A.; Binh, N.T.; Le, M.T.: Upgrading of bio-oil from biomass pyrolysis: current status and future development. In: Nanda, S., Vo, D.V.N., Sarangi, P. (eds). Biorefinery of Alternative Resources: Targeting Green Fuels and Platform Chemicals. Springer, Singapore (2020). https://doi.org/10.1007/978-981-15-1804-1_14
38. Le, M.T.; Do, V.H.; Truong, D.D.; Bruneel, E.; Van Driessche, I.; Riisager, A.; Trinh, Q.T.: Synergy effects of the mixture of bismuth molybdate catalysts with SnO_2/ZrO_2/MgO in selective propene oxidation and the connection between conductivity and catalytic activity. Ind. Eng. Chem. Res. **55**, 4846–4855 (2016). https://doi.org/10.1021/acs.iecr.6b00019
39. Zaaba, N.I.; Foo, K.L.; Hashim, U.; Tan, S.J.; Liu, W.W.; Voon, C.H.: Synthesis of graphene oxide using Modified Hummers method: solvent influence. Procedia Eng. **184**, 469–477 (2017). https://doi.org/10.1016/j.proeng.2017.04.118
40. Dogan, G.M.; Arbag, H.; Koyuncu, D.D.E.: Effect of graphene-based additives on mechanical strength and microstructure of gypsum plaster. Mater. Today Commun. **33**, 104555 (2022). https://doi.org/10.1016/j.mtcomm.2022.104555
41. Rasheed, M.; Shihab, S.; Sabah, O.W.: An investigation of the structural, electrical, and optical properties of graphene-oxide thin films using different solvents. J. Phys. Conf. Ser. **1795**, 012052 (2021). https://doi.org/10.1088/1742-6596/1795/1/012052
42. Chen, P.; Li, H.; Song, S.; Weng, X.; He, D.; Zhao, Y.: Adsorption of dodecylamine hydrochloride on graphene oxide in water. Results Phys. **7**, 2281–2288 (2017). https://doi.org/10.1016/j.rinp.2017.06.054
43. Fujimoto, H.: Theoretical X-ray scattering intensity of carbons with turbostratic stacking and AB stacking structures. Carbon **41**, 1585–1592 (2003). https://doi.org/10.1016/S0008-6223(03)00116-7
44. Chowdhury, D.R.; Singh, C.; Paul, A.: Role of graphite precursor and sodium nitrate in graphite oxide synthesis. RSC Adv. **4**, 15138–15145 (2014). https://doi.org/10.1039/C4RA01019A
45. Stobinski, L.; Lesiak, B.; Malolepszy, A.; Mazurkiewicz, M.; Mierzwa, B.; Zemek, J.; Bieloshapka, I.: Graphene oxide and reduced graphene oxide studied by the XRD, TEM and electron spectroscopy methods. J. Electron Spectrosc. Relat. Phenom. **195**, 145–154 (2014). https://doi.org/10.1016/j.elspec.2014.07.003
46. Kumar, S.; Thakur, N.: X-ray photoelectron spectroscopy and temperature-dependent electrical transport properties of $MnFe_2O_4$-reduced graphene oxide nanocomposites. Mater. Today Proc. **73**, 539–544 (2023). https://doi.org/10.1016/j.matpr.2022.10.034
47. Paul, R.; Sarkar, C.; Yan, Y.; Trinh, Q.T.; Rao, B.S.; Pao, C.W.; Mondal, J.: Porous-organic-polymer-triggered advancement of sustainable magnetic efficient catalyst for chemoselective hydrogenation of cinnamaldehyde. ChemCatChem. (2020). https://doi.org/10.1002/cctc.202000072
48. Mondal, J.; Trinh, Q.T.; Jana, A.; Ng, W.K.H.; Borah, P.; Hirao, H.; Zhao, Y.: Size-dependent catalytic activity of palladium nanoparticles fabricated in porous organic polymers for alkene hydrogenation at room temperature. ACS Appl. Mater. Interfaces **8**, 15307–15319 (2016). https://doi.org/10.1021/acsami.6b03127
49. Paul, R.; Das, R.; Das, N.; Chakraborty, S.; Pao, C.W.; Trinh, Q.T.; Peter, S.C.: Tweaking photo CO_2 reduction by altering Lewis acidic sites in metalated-porous organic polymer for adjustable H_2/CO ratio in syngas production. Angew. Chem. Int. Ed. **62**, e202311304 (2023). https://doi.org/10.1002/anie.202311304
50. Gao, X.; Jang, J.; Nagase, S.: Hydrazine and thermal reduction of graphene oxide: reaction mechanisms, product structures, and reaction design. J. Phys. Chem. C **114**, 832–842 (2010). https://doi.org/10.1021/jp909284g
51. Bollella, P.; Fusco, G.; Tortolini, C.; Sanzò, G.; Favero, G.; Gorton, L.; Antiochia, R.: Beyond graphene: Electrochemical sensors and biosensors for biomarker detection. Biosens. Bioelectron. **89**, 152–166 (2017). https://doi.org/10.1016/j.bios.2016.03.068
52. Padamata, S.K.; Yasinskiy, A.; Stopic, S.; Friedrich, B.: Fluorination of two-dimensional graphene: A review. J. Fluor. Chem. **255**, 109964 (2022). https://doi.org/10.1016/j.jfluchem.2022.109964
53. De Silva, K.K.H.; Huang, H.H.; Yoshimura, M.: Progress of reduction of graphene oxide by ascorbic acid. Appl. Surf. Sci. **447**, 338–346 (2018). https://doi.org/10.1016/j.apsusc.2018.03.243
54. Bychko, I.; Abakumov, A.; Didenko, O.; Chen, M.; Tang, J.; Strizhak, P.: Differences in the structure and functionalities of graphene oxide and reduced graphene oxide obtained from graphite with various degrees of graphitization. J. Phys. Chem. Solids **164**, 110614 (2022). https://doi.org/10.1016/j.jpcs.2022.110614
55. Zhou, Y.; Bao, Q.; Tang, L.A.L.; Zhong, Y.; Loh, K.P.: Hydrothermal dehydration for the "green" reduction of exfoliated graphene oxide to graphene and demonstration of tunable optical limiting properties. Chem. Mater. **21**, 2950–2956 (2009). https://doi.org/10.1021/cm9006603
56. Ryu, S.H.; Shanmugharaj, A.M.: Influence of long-chain alkylamine-modified graphene oxide on the crystallization, mechanical, and electrical properties of isotactic polypropylene nanocomposites. Chem. Eng. J. **244**, 552–560 (2014). https://doi.org/10.1016/j.cej.2014.01.101
57. Tai, F.C.; Wei, C.; Chang, S.H.; Chen, W.S.: Raman and X-ray diffraction analysis on unburned carbon powder refined from fly ash. J. Raman Spectrosc. **41**, 933–937 (2010). https://doi.org/10.1002/jrs.2532
58. Johra, F.T.; Lee, J.W.; Jung, W.G.: Facile and safe graphene preparation on solution-based platform. J. Ind. Eng. Chem. **20**, 2883–2887 (2014). https://doi.org/10.1016/j.jiec.2013.11.022
59. Rudenko, R.M.; Voitsihovska, O.O.; Poroshin, V.N.: Enhancement of electrical conductivity of hydrazine-reduced graphene oxide under thermal annealing in hydrogen atmosphere. Mater. Lett. **331**, 133476 (2023). https://doi.org/10.1016/j.matlet.2022.133476
60. Kartick, B.; Srivastava, S.K.: Green synthesis of graphene. J. Nanosci. Nanotechnol. **13**, 4320–4324 (2013). https://doi.org/10.1166/jnn.2013.7461
61. Saini, P.; Sharma, R.; Chadha, N.: Determination of defect density, crystallite size, and number of graphene layers in graphene analogues using X-ray diffraction and Raman spectroscopy. Indian J. Pure Appl. Phys. (IJPAP). 55, 625–629 (2017). https://doi.org/10.56042/ijpap.v55i9.16047
62. Krishnamoorthy, K.; Veerapandian, M.; Yun, K.; Kim, S.J.: The chemical and structural analysis of graphene oxide with different degrees of oxidation. Carbon **53**, 38–49 (2013). https://doi.org/10.1016/j.carbon.2012.10.013
63. Van Khai, T.; Kwak, D.S.; Kwon, Y.J.; Cho, H.Y.; Huan, T.N.; Chung, H.; Kim, H.W.: Direct production of highly conductive graphene with a low oxygen content by a microwave-assisted solvothermal method. Chem. Eng. J. **232**, 346–355 (2013). https://doi.org/10.1016/j.cej.2013.07.123
64. Wojtoniszak, M.; Chen, X.; Kalenczuk, R.J.; Wajda, A.; Łapczuk, J.; Kurzewski, M.; Borowiak-Palen, E.: Synthesis, dispersion, and cytocompatibility of graphene oxide and reduced graphene oxide. Colloids Surf. B Biointerfaces **89**, 79–85 (2012). https://doi.org/10.1016/j.colsurfb.2011.08.026
65. Trinh, Q.T.; Bhola, K.; Amaniampong, P.N.; Jerome, F.; Mushrif, S.H.: Synergistic application of XPS and DFT to investigate metal

oxide surface catalysis. J. Phys. Chem. C **122**, 22397–22406 (2018). https://doi.org/10.1021/acs.jpcc.8b05499
66. Trinh, Q.T.; Tan, K.F.; Borgna, A.; Saeys, M.: Evaluating the structure of catalysts using core-level binding energies calculated from first principles. J. Phys. Chem. C **117**, 1684–1691 (2013). https://doi.org/10.1021/jp3089758
67. Laçin, Ö.: Yeni Bir Yaklaşımla Elde Edilen Grafen Oksit Sentezlerinde SEM ve TEM Analizleri. Avrupa Bilim ve Teknoloji Dergisi. 39, 76–79 (2022). https://doi.org/10.31590/ejosat.1137870
68. Fang, X.Y.; Yu, X.X.; Zheng, H.M.; Jin, H.B.; Wang, L.; Cao, M.S.: Temperature- and thickness-dependent electrical conductivity of few-layer graphene and graphene nanosheets. Phys. Lett. A **379**, 2245–2251 (2015). https://doi.org/10.1016/j.physleta.2015.06.063
69. Jafri, S.H.M.; Carva, K.; Widenkvist, E.; Blom, T.; Sanyal, B.; Fransson, J.; Leifer, K.: Conductivity engineering of graphene by defect formation. J. Phys. D Appl. Phys. **43**, 045404 (2010). https://doi.org/10.1088/0022-3727/43/4/045404
70. Eremenko, V.V.; Sirenko, V.A.; Gospodarev, I.A.; Syrkin, E.S.; Feodosyev, S.B.; Bondar, I.S.; Minakova, K.A.: Anisotropic behavior and inhomogeneity of atomic local densities of states in graphene with vacancy groups. J. Sci. Adv. Mater. Devices. **1**, 167–173 (2016). https://doi.org/10.1016/j.jsamd.2016.06.011
71. Rao, S.; Upadhyay, J.; Polychronopoulou, K.; Umer, R.; Das, R.: Reduced graphene oxide: Effect of reduction on electrical conductivity. J. Compos. Sci. **2**, 25 (2018). https://doi.org/10.3390/jcs2020025